Preparation and Characterization of $(1-x)MgO.xSrO.Al_2O_3$ (x=0.3, 0.4, 0.5)by Co-precipitation method

Deepak Kumar Meena

Department of Ceramic Engineering
National Institute of Technology Rourkela

Preparation and Characterization of $(1-x)MgO.xSrO.Al_2O_3$ (x=0.3, 0.4, 0.5)by Co-precipitation method

Thesis submitted in partial fulfillment

of the requirements of the degree of

Master of Technology(Dual)

in

Ceramic Engineering

by

Deepak Kumar Meena

(Roll Number: 710CR1025)

based on research carried out

under the supervision of

Prof. Partha Saha

May, 2016

Department of Ceramic Engineering

National Institute of Technology Rourkela

Department of Ceramic Engineering
National Institute of Technology Rourkela

Prof. Partha Saha
Professor

May 20, 2016

Supervisor's Certificate

This is to certify that the work presented in the thesis entitled *Preparation and Characterization of* $(1-x)MgO.xSrO.Al_2O_3$ *(x=0.3, 0.4, 0.5)by Co-precipitation method* submitted by *Deepak Kumar Meena*, Roll Number 710CR1025, is a record of original research carried out by him under my supervision and guidance in partial fulfillment of the requirements of the degree of *Master of Technology(Dual)* in *Ceramic Engineering*. Neither this thesis nor any part of it has been submitted earlier for any degree or diploma to any institute or university in India or abroad.

_____
Partha Saha

Dedication

Dedicated to my parents and loved ones...

Deepak Kumar Meena

Declaration of Originality

I, *Deepak Kumar Meena*, Roll Number *710CR1025* hereby declare that this thesis entitled *Preparation and Characterization of* $(1-x)MgO.xSrO.Al_2O_3$ *(x=0.3, 0.4, 0.5)by Co-precipitation method* presents my original work carried out as a postgraduate student of NIT Rourkela and, to the best of my knowledge, contains no material previously published or written by another person, nor any material presented by me for the award of any degree or diploma of NIT Rourkela or any other institution. Any contribution made to this research by others, with whom I have worked at NIT Rourkela or elsewhere, is explicitly acknowledged in the dissertation. Works of other authors cited in this dissertation have been duly acknowledged under the sections "Reference" or "Bibliography". I have also submitted my original research records to the scrutiny committee for evaluation of my dissertation.

I am fully aware that in case of any non-compliance detected in future, the Senate of NIT Rourkela may withdraw the degree awarded to me on the basis of the present dissertation.

May 20, 2016
NIT Rourkela

Deepak Kumar Meena

Acknowledgment

Firstly, I would like to express my candid gratitude to my advisor Partha Saha sir for his encouragement, persistence and immense knowledge during the entire project work. It is an honor for me to learn from him and enrich myself as a student and a researcher.

I owe my heartfelt gratitude to the entire faculty members of Department of Ceramic Engineering for assisting me with necessary environment and technical support.

I also convey from thanks to the staff members of the Department of Ceramic Engineering for providing all the necessary support.

It would be impossible to complete my research without the support of all my family members, who has provided constant encouragement throughout my work.

Last, but not the least, I would like to thanks my friends for their constant encouragement, love, and understanding.

May 20, 2016
NIT Rourkela

Deepak Kumar Meena
Roll Number: 710CR1025

Abstract

The current study deals with the preparation and characterization of $(1-x)MgO.xSrO.Al_2O_3$ (x=0.3,0.4,0.5) based compounds by using magnesium, strontium and aluminum nitrates as oxidizers and sodium hydroxide as a precursor with co-precipitation method. XRD, SEM and FTIR analysis were performed on the calcined powders to analyze the microstructure and the phase formation of the powders. Results from XRD show the formation of $MgSrAl_{10}O_{17}$ phase upon sintering the powder at 900°C for 3h. Formation of $MgSrAl_{10}O_{17}$ phase was also observed after controlled sintering of the powder sample at 1200°C with 3h. FTIR analysis shows that symmetric or antisymmetric bending of O-Al-O network. SEM analysis of the powder sample confirmed the formation of the nanosized (20-50 nm) spherical particles. Calculated lattice parameter of $MgSrAl_{10}O_{17}$parameter(s). However, it was found with increasing x in $(1-x)MgO.xSrO.Al_2O_3$ (x =0.3, 0.4, 0.5), unit cell parameter a' increases and 'c' decreases may induces lattice strain with the neighboring minor phase(s).

***Keywords*: *Co-Precipitation*; *phosphor*; *spinel*; *lattice parameter*; *photo luminescence*.**

Contents

List of Figures

List of Tables

Chapter 1

Introduction

Magnesium–aluminum oxide $MgAl_2O_4$ is used as an important ceramic material because of its excellent mechanical strength [21], chemical inertness, high-melting point, good optical properties [13], resistivity to chemical attacks, catalytic property and excellent dielectric properties [1]. Therefore, it is widely used in certain range of applications including sensors and catalysis [2]. These excellent properties make $MgAl_2O_4$ an ideal compound for designers and engineers for use in manufacturing and processing [**?**] of numerous traditional ceramics such as, unshaped and shaped refractories for cement and metallurgical industry, armor and domes materials, photo catalyst materials, transparent windows, humidity sensors, lenses for the IR and VIS regions, dentistry materials, porous materials for high-temperature applications, and electro ceramic materials [3]. $MgAl_2O_4$ has been extensively used as refractory materials in vacuum induction furnaces, steel ladles, casting tundishes, etc [4]. It has high compressive strength at normal as well as high temperature, and exhibits no phase transition even up to the melting temperature. It is also applicable to be used as insulating materials, and optical devices. The nanosized spinel particles of $MgAl_2O_4$ [5] are highly desired in many applications because of its good chemical and physical properties .

In recent years, a variety of techniques have been adopted to produce $MgAl_2O_4$ spinel at relatively low temperatures, including precipitation, sol-gel of metal alkoxides [6], plasma-spray decomposition of oxides , ignition of urea and metal, co-precipitation [3], controlled hydrolysis of metal alkoxide, freeze drying of sulfate solutions, magnesium aluminum double alkoxide method, decomposing organometallic compounds in supercritical fluids, and aerosol method. In spite of the fact that numerous synthesis methods yielded nano-sized spinel particles [13], however, the high cost of production for generating large quantities of nanocrystalline spinel powder hinders its production in industrial scale.

Among these methods, co-precipitation route is widely used because of its simplicity, low production cost, ability to produce nano-sized powder at low temperature.

Long-lasting phosphorescent, is a phenomenon in which a phosphor when exposed to UV- radiation or sunlight shows visible luminescence for an hour or many hours in the dark. The reason for this long lasting afterglow phosphorescence is the trapping of photo-generated

electrons recombined at ionized luminescent centers when released by thermal energy [7]. These traps are deep enough to release the charge carriers at room temperature. Over past few decades, the alkaline earth aluminates long afterglow materials, in particular, dysprosium and europium co-doped strontium aluminate phosphors, are an excellent class of phosphorescence due to its long-lasting photo-luminescence, high radiation intensity, excellent thermal, chemical and radiation resistance, color purity, making it applicable in wide applications [2]. It can be used in emergency lighting, graphic arts, billboards, road signs, safe indications, escape routes, textiles and interior decorations. Additionally, it can be used in preparation of novel composite materials, and in many other forms in lamp, including CRT(cathode ray tube) and PDP (plasma display panel).

Researches on phosphors started from Palilla [6] and Abbruscato [8] who observed long lasting luminescence properties of alkaline earth aluminates in early 1960s and 1970s and it became more popular till 1990s.Presently, strontium aluminate phosphors activated by dysprosium and europium have gained much consideration because of its excellent properties. The high quantum efficiency and long lasting phosphorescence properties of $SrAl_2O_4 : Eu^{2+}, Dy^{3+}$ makes it applicable in various display devices, including, screens, glow sins, luminescent paint, detection of structural damage, etc.

Up to now, a number of synthesis methods of strontium aluminates doped with lanthanide have been described, including, solid state reaction [8], combustion method [9], sol-gel method [10], co-precipitation method, and hydrothermal method. $SrAl_2O_4 : Eu^{2+}, Dy^{3+}$ synthesized using solid-state reaction requires a high calcination temperature up to 1400 ºC to acquire a single phase. This method produced homogenous products with broad particle size distribution and low surface area. Compared with other methods, co-precipitation method is simple, energy saving and the final product with excellent luminescent properties shows smaller particle size and better distribution.

Rare-earth activated inorganic phosphors are generally used for various applications like, cathode shaft tubes, luminescent lights, X-ray radiographic screens [11]. In particular, aluminates-based phosphor gives an impression of being an astounding host material to be used in light industry. Era of light by mercury discharge was represented in early 1906 . Large number of government organizations have emphasized on new essential sources and new saving imperative advancements. SSL (solid state lightening) represents important viable advancements in lightning, offering ideal circumstances, for example, longer life span(>100,000H), and low power usage [11]. It is evaluated that the prospect of limiting half SSL was to be refined and evacuated current white-lighting developments. In any way, the existing white light emitting diodes i.e.(w-LEDs) which is made from a combination of blue LED chip and yellow-emitting phosphor cannot be used for demands of general lightening

applications because of its lower shading interpreting record (<75), and unsatisfactory high shading temperature (>4500K). A significant way to overcome these issues and get a perfect white LED that has excellent features is to use brilliant LEDs(n-UV LEDs) which emits green, red, and blue tricolor phosphors, thereby giving an outstanding and incredible higher shading rendering record, and acceptable tuned shading temperature. The blue phosphor has a higher capability due to the fact that both the blue and green phosphor can share in range of blue one. At this moment, $BaMgAl_{10}O_{17} : Eu^{2+}(BAM : Eu^{2+})$ is seen as the most favored blue-transmitting phosphor for use in w-LEDs considering the n-UV LED, however BAM exhibits a poor maintenance band around close UV range, which does not make it well sensible for current available n-UV radiating InGaN chips[12]. Therefore, it is important to analyze new blue phosphors that can be successfully and easily allowed in the n-UV region, more specifically near 400nm to increase the luminous efficiency. Aluminate based metal oxide phosphors have been found to possess good optical properties, making it an excellent material for photoluminescence applications. In past few years, work was done on the mix metal aluminates, especially Eu^{2+} - doped $MgSrAl_{10}O_{17}$ phosphor This aluminates were being prepared generally by solid state reactions, ignition and others systems, which needs high temperature. In spite of tremendous achievements, metal particle (Mn^{2+})- doped strontium magnesium hexa-aluminate ($MgSrAl_{10}O_{17}$) of β-alumina structure has gotten little attention. The β -alumina of interest for the present study is SAM.

Nowadays, strontium magnesium aluminate phosphor have gained considerable attention as an excellent luminescent material which is highly utilized in displays and lightning applications because of their extraordinary optical characteristics, thermal and chemical stability, good quantum efficiency [13]. However, for continuous enhancement of the luminescence efficiency of phosphor material to make them appropriate for white LEDs, a major breakthrough in materials front is needed. Another important concern for these phosphor used for display and lightning applications is the thermal stability, which helps in determining the reliability of devices [14]. For the above two reasons, the two properties i.e. thermal stability and luminescence efficiency needs to be considered simultaneously and needs to be enhanced by utilization of nanostructured morphology, optimizing synthesis methods, and composition.

1.1 Spinel Structure

The spinels are any class of mineral of general formulation $A^{2+}B_2^{3+}O_4^{2-}$ which crystallize in the cubic crystal system (isometric). The spinel structure is considered as a closely packed lattice of oxide ions where half of the octahedral holes and one eighth of the tetrahedral holes are occupied by metallic cations. The formula of a spinel containing two types of cations A^{n+} and B^{m+} can be written as,

$$(A_{1-2x}B_{2x})[A_{2x}B_{2-2x}]O_4$$

S.N	Aluminum Spinel	Iron Spinel	Other Spinel
1	$MgAl_2O_4$	$CuFe_2O_4$	FeV_2O_4
2	$BeAl_2O_4$	$(Fe, Mn, Zn)(Fe, Mn)_2O_4$	MgV_2O_4
3	$ZnAl_2O_4$	$MnFe_2O_4$	$(Mg, Fe)_2SiO_4$

Table 1.1: Example of different types of Spinels

The part of the formula between the parentheses represents the tetrahedral sites and the part between the brackets represents the octahedral sites. The parameter 'x' describes the degree of inversion whose value ranges from 0 to 0.5.The value x=0 represents normal spinel and the formula becomes $(A)[B_2]O_4$.The value x=0.5 represents inverse spinel and the formula becomes $(B)[AB]O_4$.Other intermediate values are found in actual cases. A and B can be divalent, trivalent, or tetravalent cations, including magnesium, zinc, iron, manganese, aluminum, chromium, titanium, and silicon. Although the anion is normally oxide, the analogous thiospinel structure includes the rest of the calcogenides.

1.1.1 Normal and Inverse Splines

The number of octahedral voids are double than tetrahedral and spinel has AB2O4 in normal spinel structure, Octahedral voids filled with trivalent atoms and the tetrahedral with divalent atoms. All trivalent cations are on octahedral sites while all divalent cations are on tetrahedral voids site. Generally spinels are symbolized by formula AB2O4and inverse spinels are symbolized by $B(AB)O_4$. Chromite and magnetite are the example of an inverse spinel.

Inverse spinel structures have another cation dissemination in that the greater part of the A cations and half of the B cations inhabit octahedral sites, while the other section of the B cations have tetrahedral sites. An occurrence of an inverse spinel is Fe_3O_4, if the $Fe^{2+}(A^{2+})$ particles are d6 high-turn and the $Fe^{3+}(B^{3+})$ particles are d5 high-turn. In development, there are reasonable conditions where the cation transport can be depicted as $(A_{1-x}B_x)[A_{x/2}B_{1-x/2}]_2O_4$, where parentheses () and bracket [] are applied to mean tetrahedral and octahedral sites, correspondingly. The supposed reversal degree, x, espouses values between 0 (normal) and 1 (inverse), and is equivalent to ⅔ for a completely arbitrary cation distribution.

Inverse spinel structures differ slightly as it takes into consideration CFSE (crystal field stabilization energy) of the metals present in the structure. Some of the ions may have different preference on the octahedral sites, which depends on the d- electron count. If the A2+ ions have a higher preference for the octahedral site, then it will force its way into that site and displace some of the B3+ ions from the octahedral site to the tetrahedral sites. Similar

if the ions have low octahedral site stabilization energy then they will have no preference and will choose the tetrahedral site. The most common example of inverse spinel is Fe_3O_4.

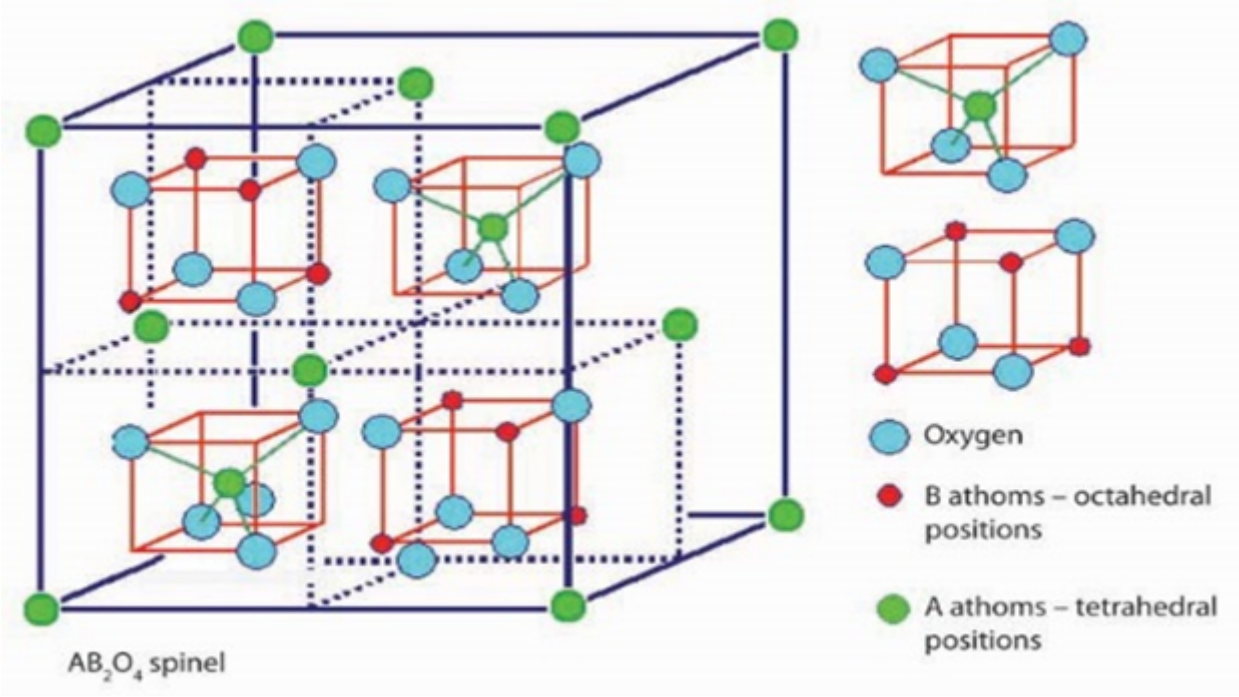

Figure 1.1: Crystal Structure of Spinel.

1.2 Applications

Rare-earth doped luminescent materials is used an important and significant radiation detectors for many applications, including radiotherapy, nuclear power plants, environmental and personal monitoring of ionizing radiation. Rare-earth doped luminescent material used in plasma display panel (PDPs), because of its good and outstanding characteristics, which includes, lower energy utilization, faster response, broad viewing angle, highly scalable, and large good quality screens. Different types of aluminates are used as hosts for doping rare earth ion in luminescent applications, such as lamp phosphors and scintillator material. Rare-earth doped BAM and SAM have been used in wide applications such as in solid-state optical device. Rare-earth doped alkaline earth aluminate phosphors has been greatly used as a material in numerous fields, including energy saving fluorescent lamps, color display screens solid state lasers, semiconductor LEDs, X-Ray medical radiography, etc.

Chapter 2

Literature Survey

Recently, a few studies have concentrated on the synthesis and characterization of doped alkaline aluminate phosphors because of their distinguished luminescent properties, for example, good stability, large quantum efficiency, durable phosphorescence and reasonable emanating color when contrasted with sulfide phosphors. These excellent properties has led to a wide potential use of the material in numerous fields, for example, low-energy fluorescent lamps, color display screens, lasers, light-emitting diodes, and X-ray and so forth. Nowadays, Strontium magnesium aluminate phosphor have pulled in much consideration as an excellent luminescent material which is highly utilized in displays and lightning applications because of their extraordinary optical characteristics, thermal and chemical stability, good quantum efficiency. We need to continuously enhance the luminescence efficiency of phosphor to make them applicable in production of efficient white LEDs. Another important concern for these phosphor used for display and lightning applications is the thermal stability, which helps in determining the reliability of devices. For the above two reasons, the two properties i.e. thermal stability and luminescence efficiency needs to be considered simultaneously and needs to be enhanced by utilization of microstructure, optimizing synthetic methods, and composition.

Jung [5] synthesized (Ba,Sr) $MgAl_{10}O_{17}$ phosphor using spray pyrolysis with particle size smaller than 1m.The luminescence properties was investigated under VUV(vaccum ultraviolet) by varying the concentration of activators. Analysis of the material revealed that by replacing Sr for Ba ,we can enhance the excitation efficiency. Moreover the luminescence intensity of (Ba,Sr)$MgAl_{10}O_{17} : Mn$ phosphor can be enhanced further by codoping it with Eu^{2+} ions.Xing et al.[15] proposed a Eu2+-doped magnesium strontium aluminate ($MgAl_{10}O_{17} : Eu^{2+}$) for PDP applications prepared using high-temperature solid state method . XRD (X-ray diffraction) characterization of the developed material found it to be a pure$MgAl_{10}O_{17}$ phase. The material emitted blue light in VUV (vaccum ultraviolet) light excitation. The phosphor showed exceptional luminescence properties even after baking it at high temperature of about $400 - 600^{o}$C.Each attribute of the material demonstrated that it would be an excellent phosphor needed for PDP applications. Later in 2008,Singh [16] prepared the Eu^{2+}-doped magnesium strontium aluminate-based phosphor ($MgAl_{10}O_{17}$:

Eu^{2+}) using low-temperature combustion method and found it to be an efficient method for preparing phosphor in a furnace which is maintained at a temperature of 500^o C for a short interval of time about a few minutes. This method as its own advantages of saving energy as well as time since the time required for preparation of phosphor is only a few minutes. Moreover, it uses urea as a fuel and nitrate as an oxidizer for the preparation which are commonly available. The synthesized material was found to be an excellent material for attaining a blue fluorescence color screens coated with phosphor.

Singh, Vijay and Chakradhar [17] successfully prepared a green light emitting phosphor $MgAl_{10}O_{17} : Mn$ using combustion method from a solution of metal nitrates. It was a one-step process without any post-annealing of the material at high temperature. The material was produced in a large scale due to the excellent potential of the oxidizer (Carbohydrazide) used in preparation. Sm3+ doped $MgAl_{10}O_{17}$ phosphor [18] was prepared using the same low-temperature combustion method. The material emitted reddish orange color emission in VUV (vaccum ultraviolet) light excitation. Pavani [11] synthesized a Dy^{3+} doped strontium magnesium aluminate (SMA) using solid stated reaction method at numerous calcination temperatures. This variation of calcination temperature helps in emission of white light which is useful for white LEDs.

Blue-light emitting $MgXAl_{10}O_{17} : Eu^{2+}$ phosphor X= (Sr, Ca) [19] was synthesized successfully by using the combustion method in a furnace maintained at 500^oC under UV and UV excitation wavelength. The emission of blue light occurs around 469 nm and 452 nm which was found to be closer to UV-region. This near UV-excited phosphor can be utilized for fabrication of white-LEDs. For usage in optical telecommunication and wavelength multiplexing applications, a fierce infrared emitting $MgSrAl_{10}O_{17} : Er^{3+}$phosphor co-doped with Yb^{3+}, Ba^{2+} and Ca^{2+}ions [20]was prepared through solution combustion method. The material was excited at 980 nm to observe the wide and intense infrared emission of Er3+ ions. Later on, Aluminate phosphors $SrMgAl_{10}O_{17}$ co-doped with Eu^{2+} and Mn^{2+} ions[21] was synthesized using solid-state reaction method. The color emitted by phosphorous can be varied from cyan to green by varying the concentration ratios of Eu^{2+} and Mn^{2+} ions. Strong absorption property exhibited by this phosphors make it applicable for white LEDs as UV-convertible phosphors.

The superior features exhibited by W-LED (white light emitting diodes) makes it applicable for future-generation lightning material used in phones, cars, traffic lights, and some daily life uses. Creation of a warm W-LED has motivated researchers to explore efficient red phosphorus. To accomplish these needs a red colored aluminate phosphors $SrMgAl_{10}O_{17}$ doped with Mn^{4+} ions[2] was synthesized using solid-state reaction in a furnace maintained at a temperature of 1400^oC.XRD characterization of the synthesized material showed that this material incorporates only a single phase and there is no impure

phase present in it. The spectrum of $SrMgAl_{10}O_{17} : Eu^{4+}$ showed that it could be excited by two spectrum of light, one is near ultraviolet light and other is with the blue light emitted from diode chips. According to the evaluation all the ions i.e. Li^{+}, Na^{+}, and Cl^{-} can enhance the luminescent properties of $SrMgAl_{10}O_{17} : Mn^{4+}$ which makes it suitable to be utilized as a red component in warm white light-emitting diodes used in various types of lightning applications.

Several studies have been done on rare-earth ions doped $SrMgAl_{10}O_{17}$ but reports on transition metal ions doped $SrMgAl_{10}O_{17}$ is not in much detailed. The interest of attaining new photo-luminescent products has motivated the study of optical properties of transition metal ions. Amongst the various existing transition metal ions, Cr^{3+} is more impressing for spectroscopic researches because of its sensitivity and dynamic behavior. For these reasons,$SrMgAl_{10}O_{17} : Cr^{3+}$phosphor[22] was prepared using combustion method in a furnace maintained at 500^{o}C for a short interval of time (< 5 minutes).XRD of the phosphor found it to have a single phase without the presence of any impure phase even at low temperature of about 500^{o}C. The evaluation of this phosphor shows that Cr^{3+} ions are used strongly in field sites. A pure-phase and high-splendor blue phosphor $SrMgAl_{10}O_{17} : Eu^{2+}$ doped (SAM)[23] was prepared using a hybrid ureasol combustion method at a temperature as low as 600^{o}C. Hybrid method has led to considerable increase in luminescence by 52.2% and an increase in thermal stability by 8.8% at 435k as compared to the traditional combustion method. This blue phosphor prepared by hybrid method can be utilized for near ultraviolet light emitting diodes.

Doped luminescent samples have a significant place as radiation detectors in a number of fields, including, radiotherapy, nuclear plants, geological dating, and monitoring of ionizing radiation. Thermoluminescence (TL) means the ejection of light which is beyond the thermal equilibrium because of large absorption of energy from external sources. Recently, this property has been studied and investigated by several researchers. Mechanoluminescence (ML) and Thermoluminescence (TL) characteristics of $SrMgAl_{10}O_{17} : Eu^{2+}$ phosphor prepared using combustion method [24] was investigated under gamma irradiation. Luminescence emission spectrum of the phosphor showed a higher peak at 460nm.Evlaution of TL properties shows a liner increase up to 1770 Gamma dose, which makes it applicable in gamma ray dosimetry.

2.1 Objective of the Thesis

- Preparation of $MgSrAl_{10}O_{17}$ compound using stoichiometric mixture of $(1-x)MgO : xSrO : Al_2O_3$ (x = 0.3, 0.4, 0.5) by co-precipitation route using aluminum, magnesium and strontium nitrates as precusors.
- Phase analysis by X-ray diffraction and calculation of lattice parameters.

- Microstructural characterization by FESEM.
- Determination of atomic vibration and optical properties using FTIR and UV-visible spectroscopy.

Chapter 3

Materials and Methodology

3.1 Chemicals Used

Magnesium nitrate hex-hydrate AR (Merck Ltd.), Aluminium nitrate nonahydrate (Loba Chemie Pvt. Ltd), Strontium nitrate (s.d fine- chem pvt. ltd.) and 1M NaOH solution (Precipitating agent).

3.2 Batch calculation

The batch was calculated using the stoichiometric mixture of $(1-x)MgO : xSrO : Al_2O_3$ (x = 0.3, 0.4, 0.5) and mentioned in Table 3.1. Figure 3.1 shows the flowcharts diagram of the synthesis method.

Composition	$Mg(NO_3)_2.6H_2O(g)$	$Sr(NO_3)_2(g)$	$Al(NO_3)_2.9H_2O(g)$
$0.7MgO.0.3SrO.Al_2O_3$	17.94	6.34	37.56
$0.6MgO.0.4SrO.Al_2O_3$	15.38	8.46	37.56
$0.5MgO.0.5SrO.Al2O3$	12.82	10.58	37.56
$MgO.Al_2O_3$	10	–	14.64
$SrO.Al_2O_3$	–	10	17.74

Table 3.1: Batch Composition

3.3 Experimental Procedure

First we prepared $Mg(NO_3)_2.6H_2O, Sr(NO_3)_2 and Al(NO_3)_3.9H_2O$ solution in distilled water in separate beaker at the same time. 1M NaOH solution was prepared and maintained at 60^oC then the solutions were poured into sodium hydroxide solution drop wise. Immediately, after that, the solution turned turbid, and a colloidal white precipitate solution was observed. In addition, 20-30 ml of NH_4OH was added to incipient preparation. The precipitate was settled for 12h and filtered using filter paper. The solid cake was washed with distilled water and ethanol few times before drying in hot air oven at 100^oC for 10 hours. The dried mass was calcined in an aluminum crucible at 900^oC and 1200^oC for 3 hours duration. After,

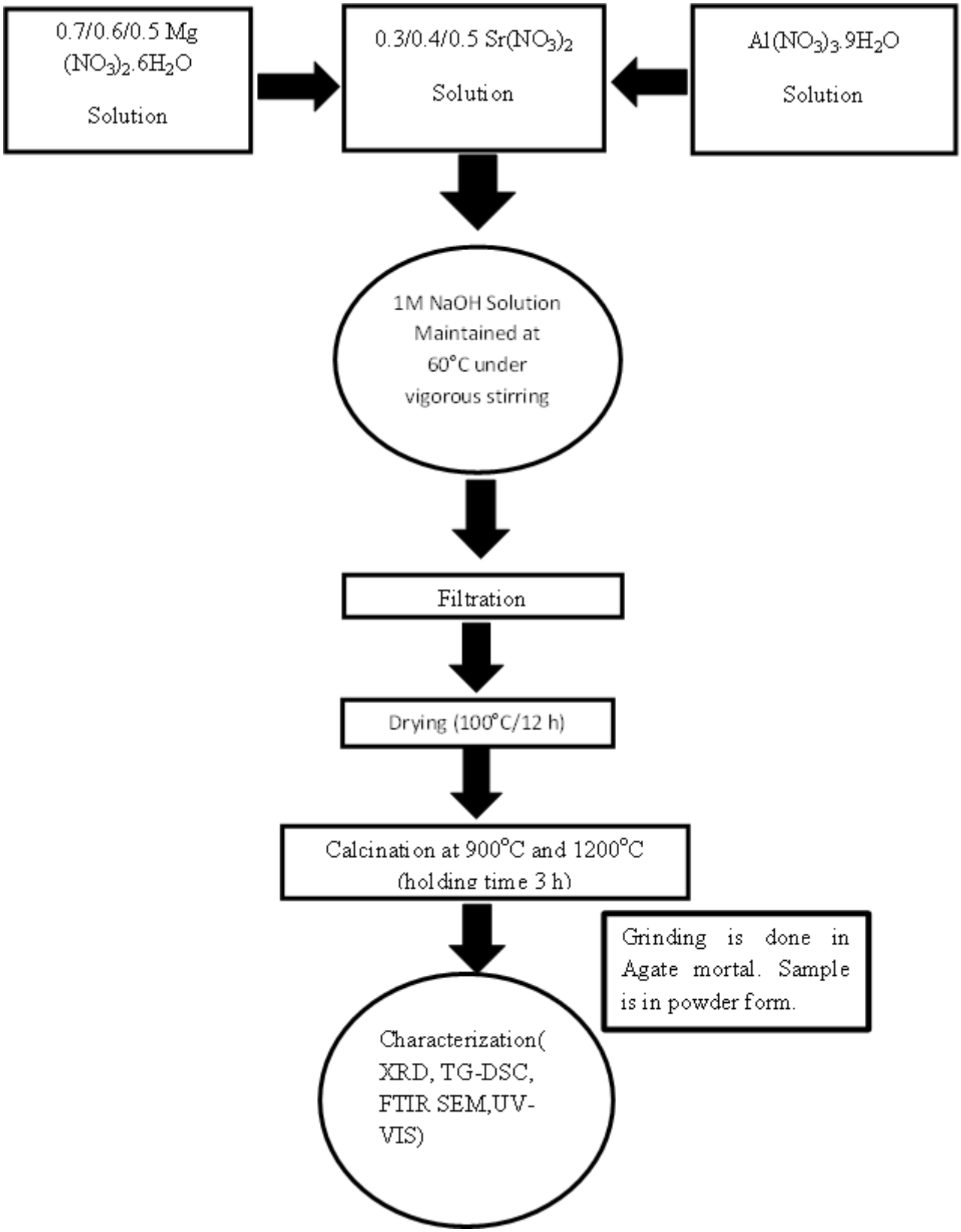

Figure 3.1: Flowchart for the synthesis of (1-x)$MgO.xSrO.Al_2O_3$ stoichiometric compound

calcination, the agglomerated powder was crushed in agate mortar and used for various

characterization.

3.4 Material Characterizations

The calcined powders were characterized using TG-DSC, XRD, FESEM, FTIR, and UV-visible spectroscopy.

3.4.1 Differential Scanning Calorimetry and ThermoGravimetry Test

The thermal profile of $MgAl_2O_4$ sample was determined using Netzsch STA 449C thermal analyzer (Netzsch, Germany) at a constant heating rate of 10°C/min in the temperature range of 30°C to 1000°C in air.

3.4.2 XRD Analysis of Calcined Powders

The powder XRD pattern of the calcined powders was acquired using Co Kα (λ = 1.789Å) radiation (Bruker D8 Advance) within 2 value of 10-80□ with 0.05□ step size. The observed XRD pattern was indexed using standard ICDD files found in the PANalytical X'Pert HighScore Plus database and the unit cell parameter(s) were determined using CEL software based on least-square method.

3.4.3 Field Emission Scanning Electron Microscope (FESEM) study

SEM micrographs of the calcined powder samples were recorded at different magnifications using field emission scanning electron microscope (NOVA NANOSEM FEI450) operating at 30 kV. First, powder samples were spread onto carbon tape followed by sputter coating with gold for 4 min in order to avoid charge build-up during the FESEM microstructural analysis.

3.4.4 Fourier Transform Infrared spectroscopy (FTIR)

The chemical structure of the calcined powders was determined by Fourier Transform Infra-Red Spectroscopic (FTIR) analysis. The powder samples were mixed with KBr (1:10 wt. % ratio) and pellets were pressed. FTIR spectra of the pellets was recorded (Perkin Elmer Spectrum version 10.4.00, model number 95277) between wave number ranges of 450 to 4000 cm-1 at room temperature. A reference pellet of KBr was also used to cancel out the FTIR spectra of KBr from the desired powder sample.

3.4.5 Ultraviolet Visible

The UV-visible absorption of the samples was measured at room temperature by diffuse reflectance spectroscopy using a Lambda 35, Perkin Elmer UV-visible spectrophotometer

equipped with an integrating sphere.

Chapter 4

Results and Discussion

TG DSC analysis

The Fig 4.1 represents the DSC-TG curve of $MgAl_2O_4$ powder obtained by calcination at 900°C for 3h of the powders mixed by solid state methods using metal nitrates precursors. From the TG-DSC curve it appears that at 112°C, an endothermic peak was observed due to the removal of physically adsorbed water [ref.]. At about 300°C another endothermic peak was evident which corresponds to 25% loss in mass due to the removal of crystalline water present in the precursor during synthesis.

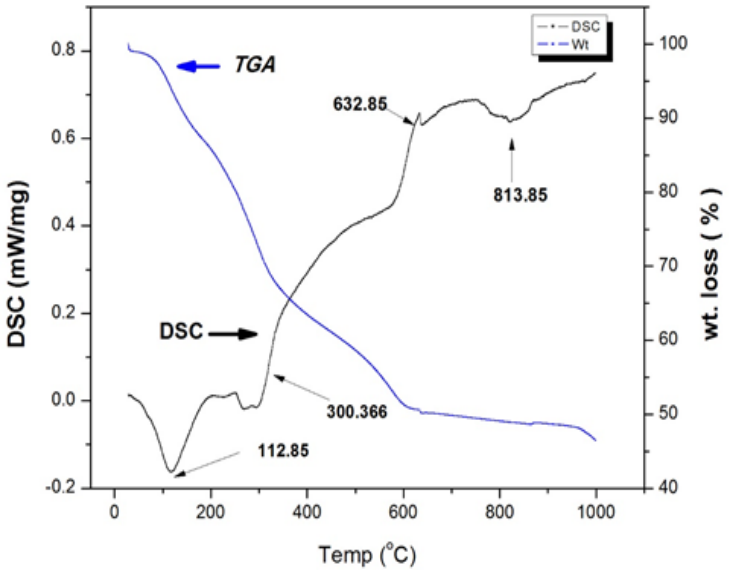

Figure 4.1: TG-DSC curves for $MgAl_2O_3$ fired at 900^oC for 3h

A single exothermic peak was observed at 633^oC due to the braking of bonds in the structure. The last endothermic peak obtained at 813^oC was mainly due to onset of spinel formation [ref.]. There was a rapid mass loss of 45% from the room temperature to 633^oC, which clearly manifest the decomposition of nitrates present in the sample. There was a negligible weight loss beyond the temperature of 633°C to till 1000°C suggest the formation of spinels.

XRD analysis

$MgAl_2O_4$ formed at 900^oC and 1200^oC for 3h

The figure 4.2 represent the XRD patterns of $MgAl_2O_4$ which was formed by solid state synthesis method using $Mg(NO_3)_2$ and $Al(NO_3)_3$ at two different temperature of 900^oC and 1200^oC for 3h. The upper curve shows the XRD pattern of 900^oC/3h sample and the lower curve represent the XRD pattern of $MgAl_2O_4$formed by calcination at1200^oC for 3h. It can be seen that $MgAl_2O_4$ (spinel) was found as major phase and MgO (periclase) and Al_2O_3 (corundum) as minor phase(s) in both the samples. In is also apparent that phase pure MgAl2O4 was not formed and corundum and periclase appeared as. Increase in temperature to 1200^{o}C confirms the spinel phase for the given compositions. Calculated lattice parameter of MgAl2O4 calcined at 900°C for 3h (a = 8.08 Å, unit cell volume 528.46 Å3) and 1200°C 3h (a = 8.06 Å, and unit cell volume 524.43 Å3) matched quite well with the standard lattice parameter of $MgAl_2O_4$ spinel (a = 8.09 Å, and unit cell volume 528.89 Å3)

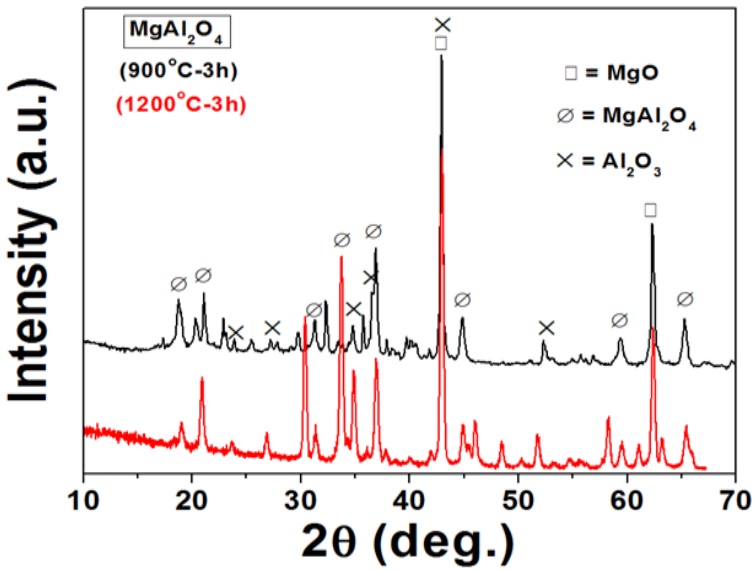

Figure 4.2: XRD for $MgO.Al_2O_3$ fired at two different temperature that are 900^{o}C and 1200^{o}C for 3 h

$SrO.Al_2O_3$ formed at 1200^{o}C for 3h

The figure 4.3 shows the XRD pattern of $SrAl_2O_4$ which was formed by calcination at 1200^oC for 3h of the hydroxide precipitate formed room temperature. From the figure it could be observed that $SrAl_2O_4$ (spinel) was obtained as major phase. Calculated lattice parameter of $SrAl_2O_4$ (a = 5.16 Å, b = 8.85Å, c= 8.45 Å, and unit cell volume 385.46 Å3) matched well with the standard lattice parameter of $SrAl_2O_4$ spinel (a = 5.16 Å, b = 8.82Å, c= 8.44 Å, and unit cell volume 383.70 Å3).

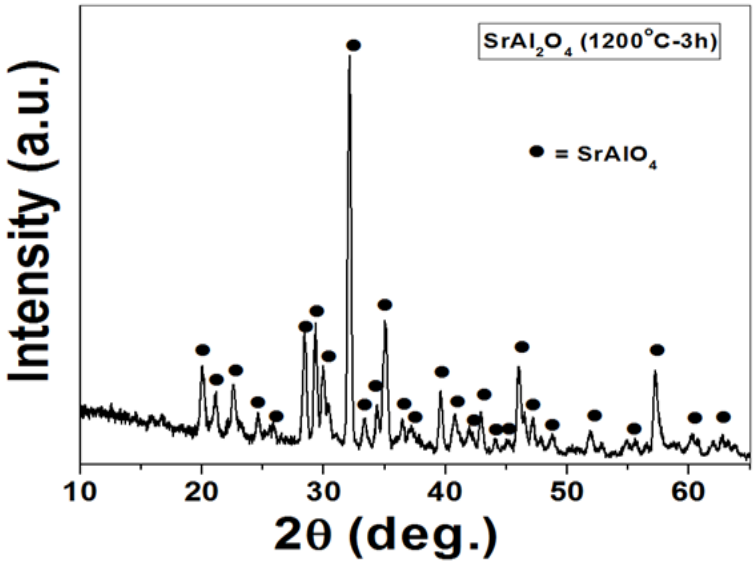

Figure 4.3: XRD for $SrO.Al_2O_3$ fired at 1200^{o}C for 3 h

$0.5MgO.0.5SrO.Al_2O_3$ calcined at 900^{o}C for 3h

The figure 4.4 shows the XRD pattern of $0.5MgO.0.5SrO.Al_2O_3$ powder sample which was calcined at 900^{o}C for 3h. It can be observed that desired $MgSrAl_{10}O_{17}$ was formed as major phase and MgO and $SrAl_2O_4$ were formed as minor impurities. Calculated lattice parameter of $MgSrAl_{10}O_{17}$ (a = 5.91 Å, c= 22.39 Å, and unit cell volume 676.58 Å3) shows good trend with standard lattice parameter of $MgSrAl_{10}O_{17}$ (a = 5.63 Å, c= 22.36 Å, and unit cell volume 612.89 Å3).

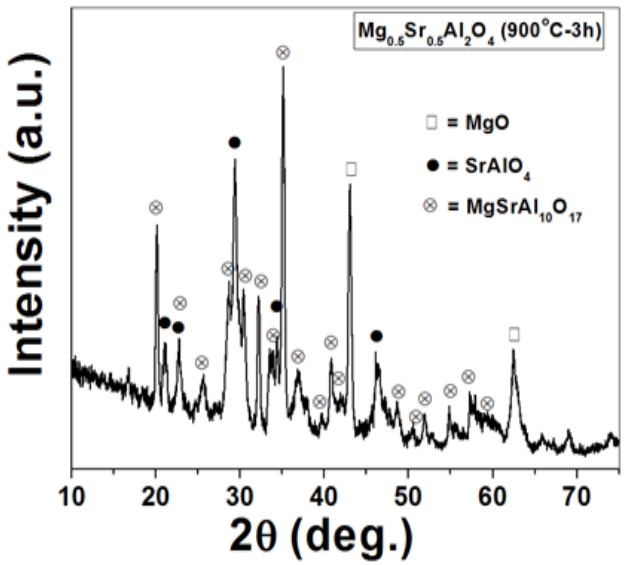

Figure 4.4: XRD for $0.5MgO.0.5SrO.Al_2O_3$ fired at 900^{o}C for 3 h

$0.6MgO.0.4SrO.Al_2O_3$ calcined at 900^oC and 1200^oC for 3h

The figure 4.5 represents the XRD patterns of $0.6MgO.0.4SrO.Al_2O_3$ powder sample which was calcined at900^oC for 3h. The major phase $MgSrAl_{10}O_{17}$ was observed along with MgO as minor phase. However, the same sample upon calcination at 1200^oC for 3h

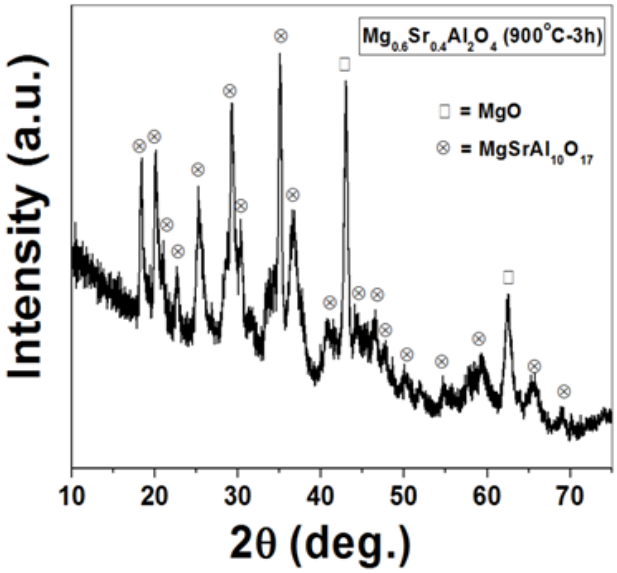

Figure 4.5: XRD for $0.6MgO.0.4SrO.Al_2O_3$ fired at 900^oC for 3h

shows the formation of $MgSrAl_{10}O_{17}$ and $SrAl_2O_4$ and MgO as secondary phase(s) [see figure(4.6)]. So, it appears that at high temperature an additional phase $SrAl_2O_4$ was formed. Calculated lattice parameter of $MgSrAl_{10}O_{17}$ formed at 900^oC for 3h (a = 5.71 Å, c= 20.13 Å, and unit cell volume 568.59 Å3) $MgSrAl_{10}O_{17}$ formed at 1200^oC for 3h (a = 5.99 Å, c= 21.65 Å, and unit cell volume 673.28 Å3) shows decent trend with standard lattice parameter of$MgSrAl_{10}O_{17}$ (a = 5.63 Å, c= 22.36 Å, and unit cell volume 612.89 Å3).

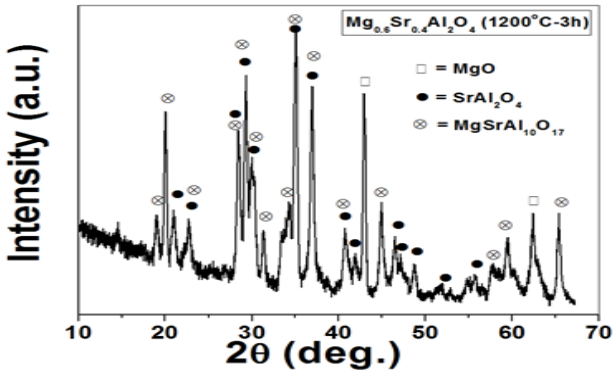

Figure 4.6: XRD for $0.6MgO.0.4SrO.Al_2O_3$ fired at 1200^oC for 3h

$0.7MgO.0.3SrO.Al_2O_3$ calcined at 900^oC for 3h

Figure 4.7 shows the XRD pattern of $0.7MgO.0.3SrO.Al_2O_3$ stoichiometric composition calcined at 900°C for 3h. It could be observed that $MgSrAl_{10}O_{17}$ was found as major phase and MgO (periclase) and Al_2O_3 (corundum) as minor phase(s). Calculated lattice parameter of $MgSrAl_{10}O_{17}$ (a = 5.91 Å, c= 22.39 Å, and unit cell volume 676.58 Å3) shows good trend with standard lattice parameter of $MgSrAl_{10}O_{17}$ (a = 5.63 Å, c= 22.36 Å, and unit cell volume 612.89 Å3). So, it is clearly apparent that changing the MgO/SrO or Mg^{2+}/Sr^{2+} ratio has direct consequences on the phase formation. When, Mg^{2+}/Sr^{2+} ratio increased from 1 to 1.5, the secondary phase(s) $SrAl_2O_4$ completely disappeared and only MgO was found. Similarly, when the Mg^{2+}/Sr^{2+} ratio changed from 1.5 to 2.3 additional phase corundum (Al_2O_3) appeared in addition the MgO (periclase) phase. So, it is obvious that MgO phase has the preference was formed for all the three studied composition as a secondary phase.

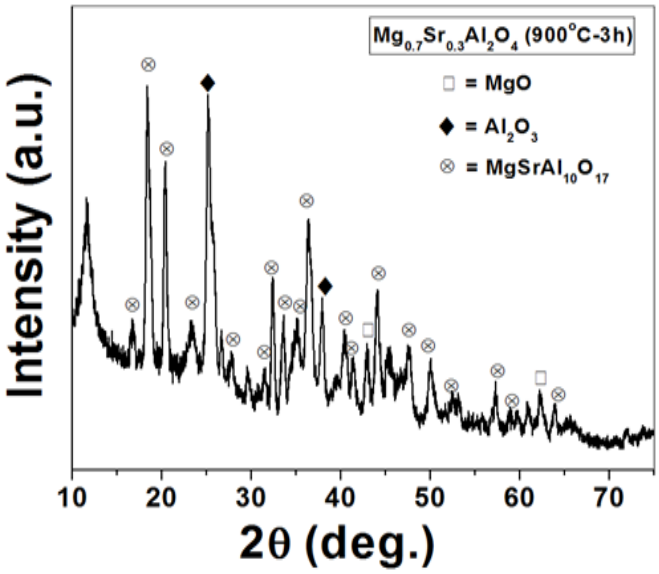

Figure 4.7: XRD for $0.7MgO.0.3SrO.Al_2O_3$ fired at 900^oC for 3 h

Lattice parameter(s) calculation from XRD patterns

From the Table 4.1 it appears that calculated lattice parameter of $MgSrAl_{10}O_{17}$ (crystal system: Hexagonal, space group: P63/mmc, space group number: 194) show good match with the standard lattice parameter(s). With increasing x in $xMgO.(1-x)SrO.Al_2O_3$ (x = 0.5, 0.6, 0.7) compositions, unit cell parameter 'a'increases and 'c' decreases of $MgSrAl_{10}O_{17}$ suggest that c/a ratio decreases in the samples compared to standard c/a value. The decrease in c/a value may imparts lattice strain or crystal clamping with the neighboring minor phase(s)

Sample Name	No of Phases found	Standard Lattice Parameters of Major Phase a(A)	b(A)	Volume(A^O)	Calculated Lattice Parameters of Major Phase a(A)	b(A)	Volume(A^O)
$0.5MgO.0.5SrO.Al_2O_4$ heat treated at 900°C for 3h	$MgSrAl_{10}O_{17}$(major) MgO(minor) $SrAl_2O_4$(minor)	5.63	22.36	612.89	5.91	22.39	676.58
$0.6MgO.0.4SrO.Al_2O_4$ heat treated at 900°C for 3h	$MgSrAl_{10}O_{17}$(major) MgO(Minor)	5.63	22.36	612.89	5.71	20.13	568.59
$0.7MgO.0.3SrO.Al_2O_4$ heat treated at 900°C for 3h	$MgSrAl_{10}O_{17}$(major) MgO(Minor) Al_2O_3(minor)	5.63	22.36	612.89	5.91	20.14	608.71
$0.6MgO.0.4SrO.Al_2O_4$ heat treated at 1200°C for 3h	$MgSrAl_{10}O_{17}$(major) MgO(Minor) $SrAl_2O_4$(Minor)	5.36 5.16 b=8.82	22.36 8.44	612.89 383.70	5.99 5.15 b=8.84	21.65 8.44	673.28 383.85
$SrAl_2O_4$ heat treated at 1200°C for 3h	$SrAl_2O_4$	5.16 b=8.82	8.44	383.70	5.16 b=8.85	8.45	385.46
$MgAl_2O_4$ heat treated at 900°C for 3h	$MgAl_2O_4$(major) MgO(Minor) $SrAl_2O_3$(Minor)	8.09	—-	528.89	8.08	—	528.46
$MgAl_2O_4$ heat treated at 1200°C for 3h	$MgAl_2O_4$(major) MgO(Minor) $SrAl_2O_3$(Minor)	8.09	—-	528.89	8.06	—	524.43

Table 4.1: Standard and calculated unit cell parameter(s) determined from XRD analysis

Microstructural Analysis

$MgO.Al_2O_3$ formed at 900^oC for 3h

SEM micrographs of the $MgAl_2O_4$ formed at 900^oC for 3h with low and high magnification are shown in figure 4.8. Most of the particles took the form of non-uniform spherical shape. High-resolution SEM micrographs show the presence of several micro- and nanoparticles within the grains. Average particle size was measured 98 .

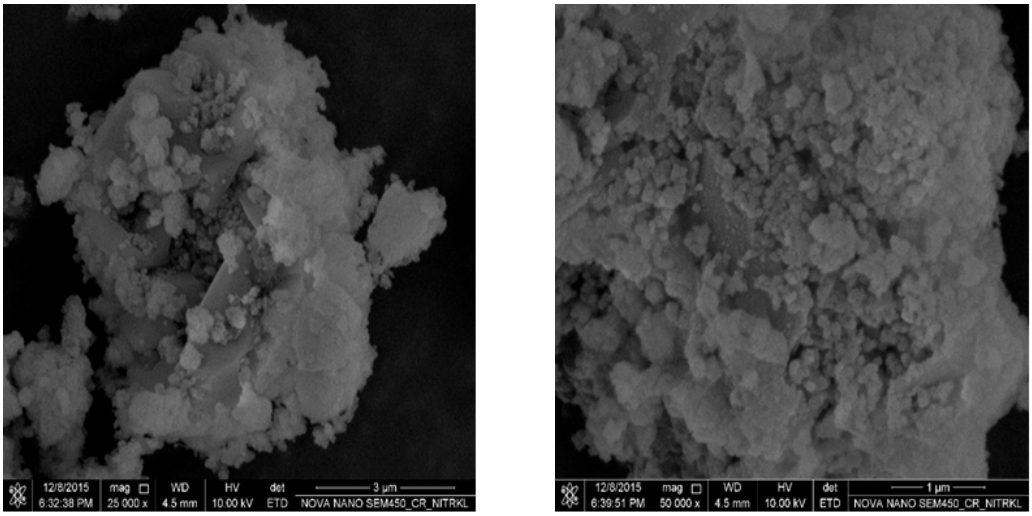

(a) (b)

Figure 4.8: FESEM images for $MgO.Al_2O_3$ fired at 900^OC for 3h

$MgAl_2O_4$ formed at 1200^0C for 3h

Figure 4.9 show the SEM micrographs of the sample calcined at 1200^0C for 3h. SEM images show that particles are agglomerated. Spinel particles in the form of hexagonal platelets were found. Average particle size were found submicron to 2 in size.

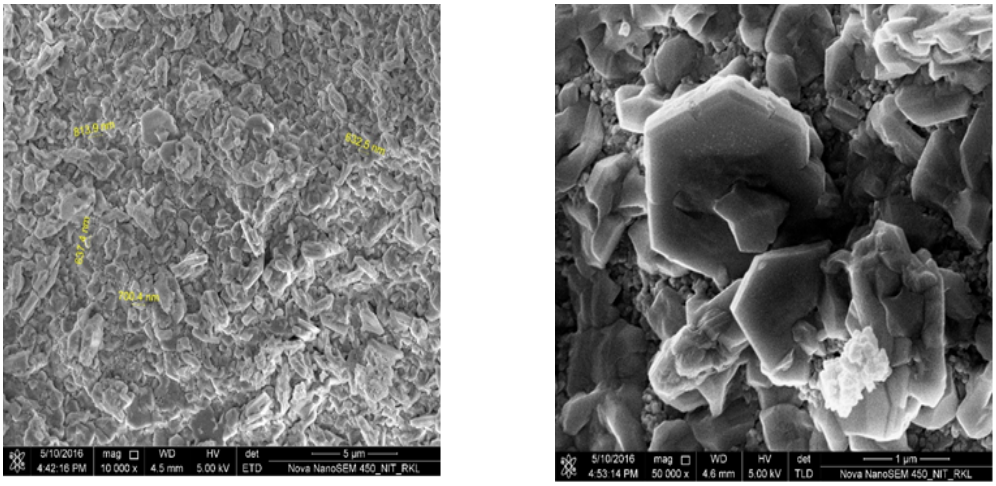

(a) (b)

Figure 4.9: FESEM images for $MgO.Al_2O_3$ fired at 1200^OC for 3h

$SrO.Al_2O_3$ formed at 1200^{o}C for 3h

SEM image of $SrAl_2O_4$ formed at 1200^{o}C for 3h is illustrated in in figure 4.9. The SEM image shows the presence of several micron size particles. The particles possess interconnected globules-like morphology with agglomerated structures. The average crystallite size was measured 77 microns.

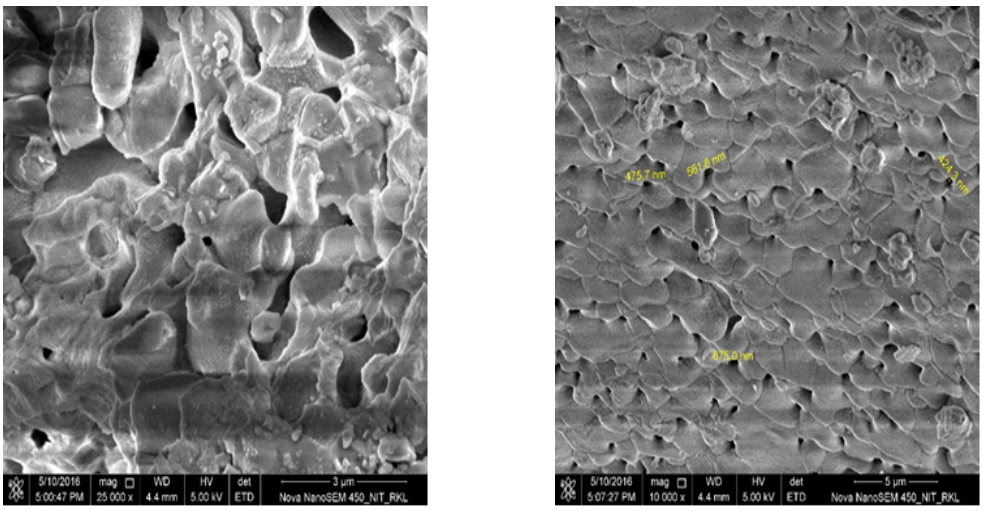

(a) (b)

Figure 4.10: FESEM images for $SrAl_2O_4$ fired at 1200^OC for 3h

$0.5MgO.0.5SrO.Al_2O_3$ calcined at 900^oC for 3h

Figure 4.10 show the SEM images of $0.5MgO.0.5SrO.Al_2O_3$ sample calcined at 900^oC for 3h. It is clearly seen that loosely agglomerated particles were formed. Particles were in nanometer size with average particle size 21 nm.

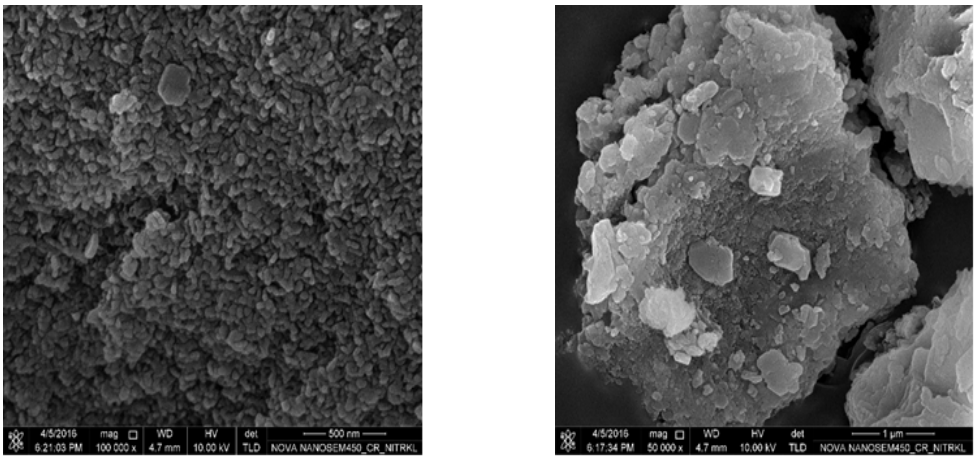

(a) (b)

Figure 4.11: FESEM images for $0.5MgO.0.5SrO.Al_2O_3$ fired at 900^OC for 3h

$0.6MgO.0.4SrO.Al_2O_3$ calcined at 900^oC for 3h

From the SEM image, it can be observed that the crystallites have non uniform morphology. SEM micrographs show the presence of nanoparticles with average size 100 nm [see figure(4.11)].

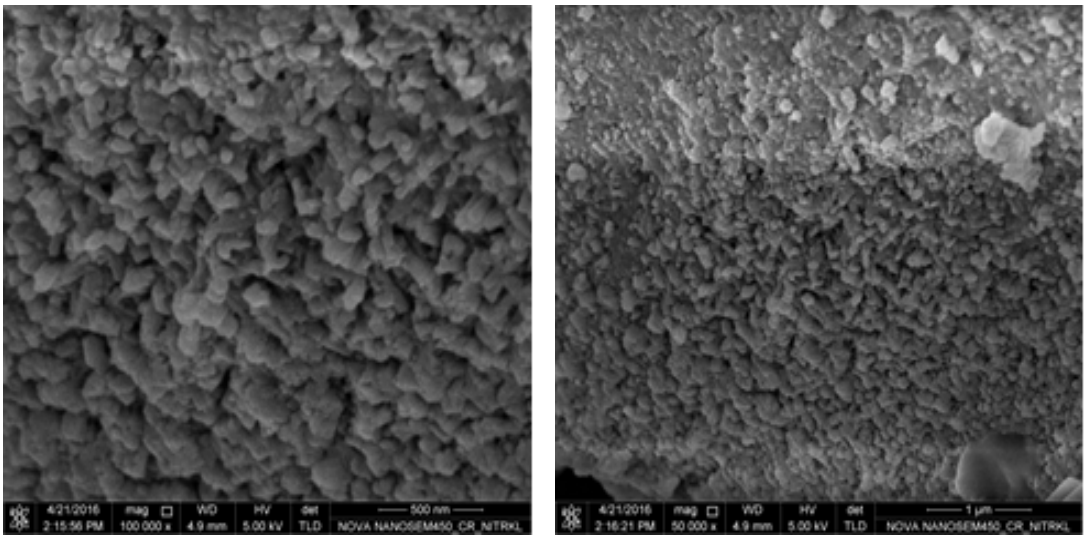

(a) (b)

Figure 4.12: FESEM images for $0.6MgO.0.4SrO.Al_2O_3$ fired at 900^OC for 3h

$0.7MgO.0.3SrO.Al_2O_3$calcined at 900^oC for 3h

Figure 4.12 show the SEM images of $0.7MgO.0.3SrO.Al_2O_3$ calcined at 900^oC for 3h samples. For $0.7MgO.0.3SrO.Al_2O_3$, the average crystallite size was calculated 83 nm. Particles were nearly spherical in nature. From the SEM image it appears that particles are loosely agglomerated likely due to formation of periclase, alumina and the $MgSrAl_{10}O_{17}$ at different temperature during firing. The phase which was formed early may assisted to from liquid-phase during sintering of the remaining phase(s).

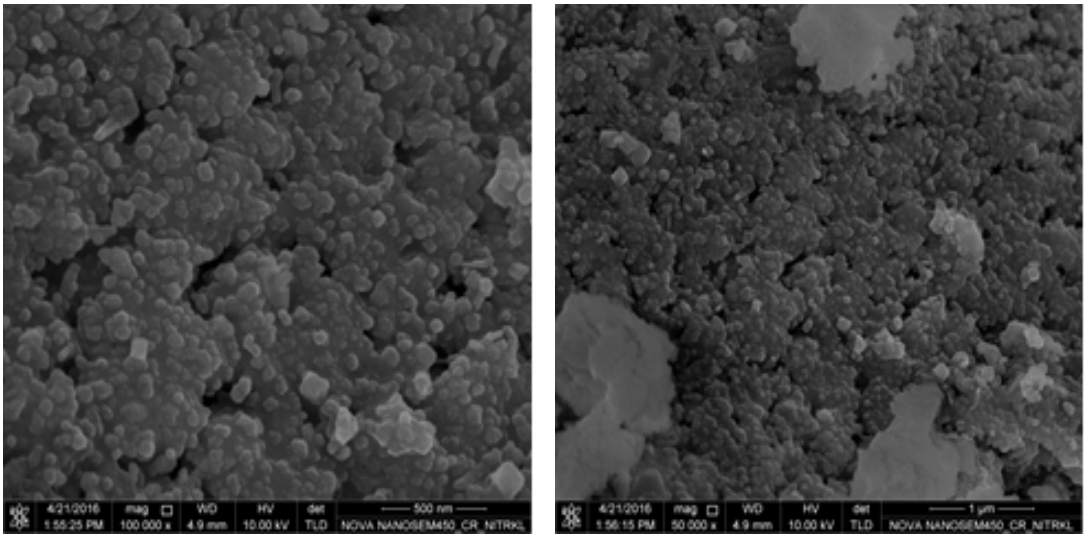

(a) (b)

Figure 4.13: FESEM images for $0.7MgO.0.3SrO.Al_2O_3$ fired at 900^OC for 3h

$0.5MgO.0.5SrO.Al_2O_3$ calcined at 1200^OC for 3h

The figure 4.13 shows the fully agglomerated particles with non-uniform morphology of the calcined sample. It can be seen with increase the calcination temperature from 900°C to 1200°C has direct consequences on the resultant microstructure. Average particle size was 500-600nm

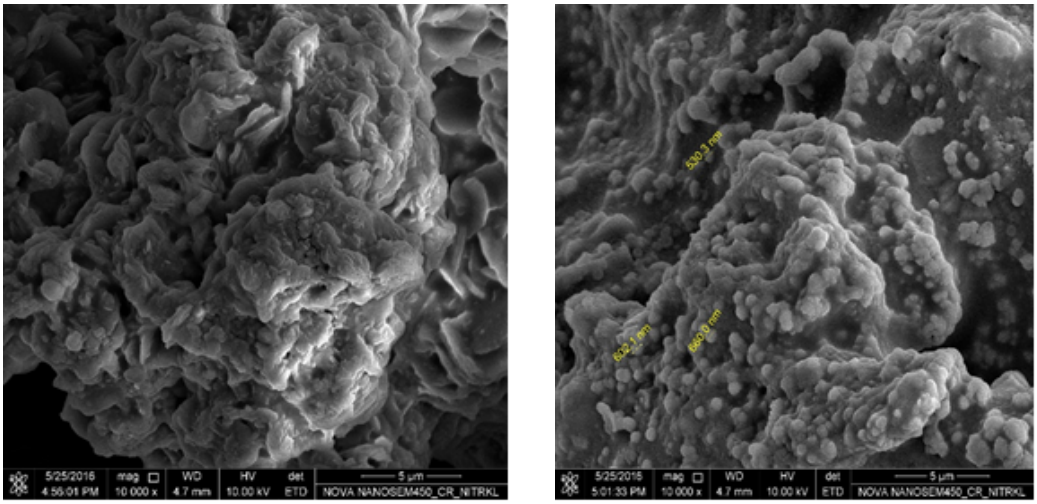

(a) (b)

Figure 4.14: FESEM images for $0.5MgO.0.5SrO.Al_2O_3$ fired at 1200^OC for 3h

$0.6MgO.0.4SrO.Al_2O_3$ calcined at 120^OC for 3h l

The sample calcined at 1200^OC, shows 5-7 agglomerated particles in SEM image. It can be seen with increase in firing temperature from 900°C to 1200°C has direct consequences on the resultant microstructure. Particle size increases from 100 nm to 5-7 ẘith increase in temperature from 900°C to 1200°C.

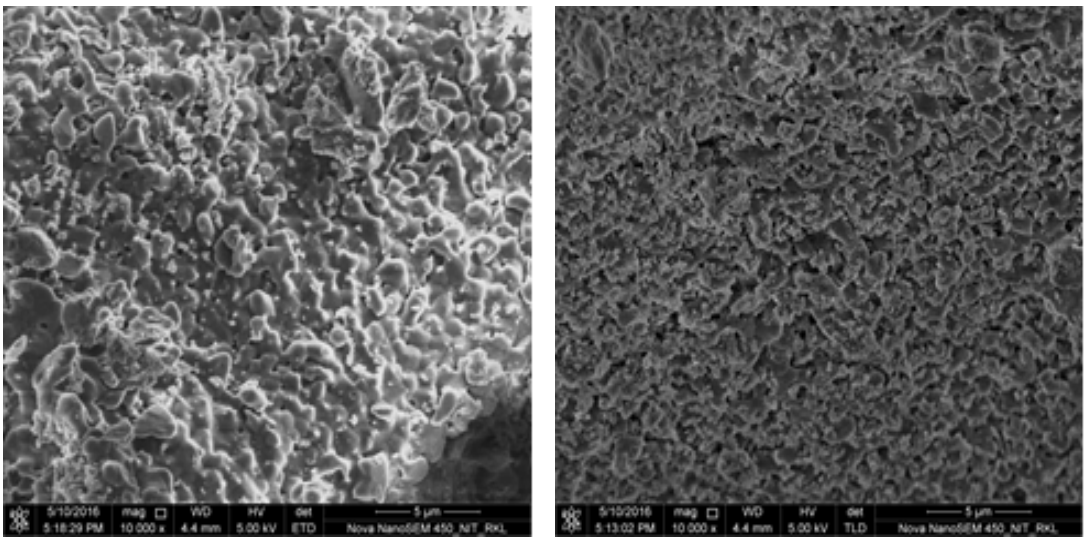

(a) (b)

Figure 4.15: FESEM images for $0.6MgO.0.4SrO.Al_2O_3$ fired at 1200^OC for 3h

$0.7MgO.0.3SrO.Al_2O_3$ calcined at 1200^OC for 3h

From the figure 4.13 it can be observed the formation foamy agglomerated structure of particles. Most of the particles took the form of irregular shape. High-resolution SEM micrographs show the presence of several micron size particles agglomerated with each other. Average particle size was measured 0.5 μ.

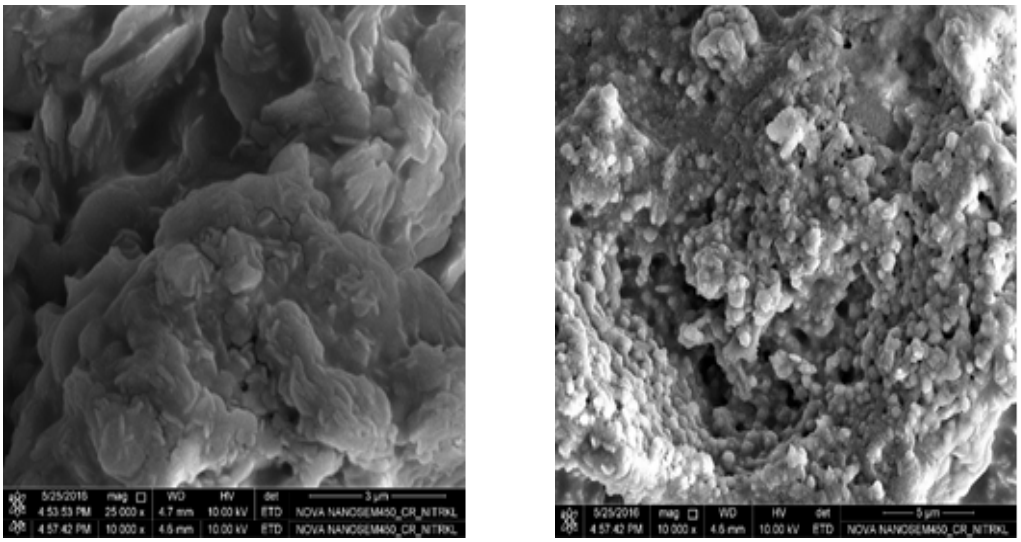

(a) (b)

Figure 4.16: FESEM images for $0.7MgO.0.3SrO.Al_2O_3$ fired at 1200^OC for 3h

FTIR Spectra

$0.7MgO.0.3SrO.Al2O3$ calcined at 900^oC for 3h

The FTIR spectra in figure 4.14 shows absorption band in different regions; the peak at about 1464 cm^{-1} arising from the bending vibration of Mg-O and peak at $1028cm^{-1}$ which is due to the Al-O vibrations in the spinel structure. Further, in the 400-1028 cm^{-1} region of the IR spectrum, the observed specific sharp, distinct and intense peaks are attributed to the characteristics metal-oxygen vibrations.

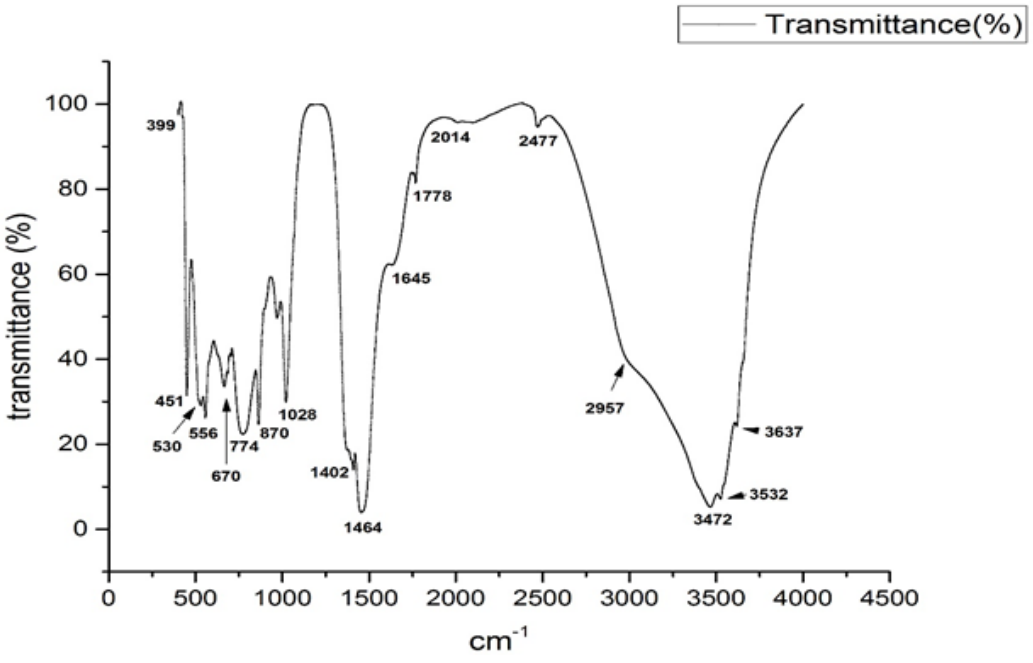

Figure 4.17: FTIR Spectra of $0.7MgO.0.3SrO.Al_2O_3$ fired at 900^OC for 3h

$0.6MgO.0.4SrO.Al_2O_3$ calcined at 900^oC for 3h

The FTIR spectra shown figure 4.15 illustrate absorption band in different regions: the peak at about 1464 cm^{-1} arising from the bending vibration of Mg-O and peak at 1028 cm^{-1} which is due to the Al-O vibrations in the spinel structure. Further, in the 513-879 cm^{-1} region of the IR spectrum, the observed specific sharp, distinct and intense peaks are attributed to the characteristics metal-oxygen vibrations.

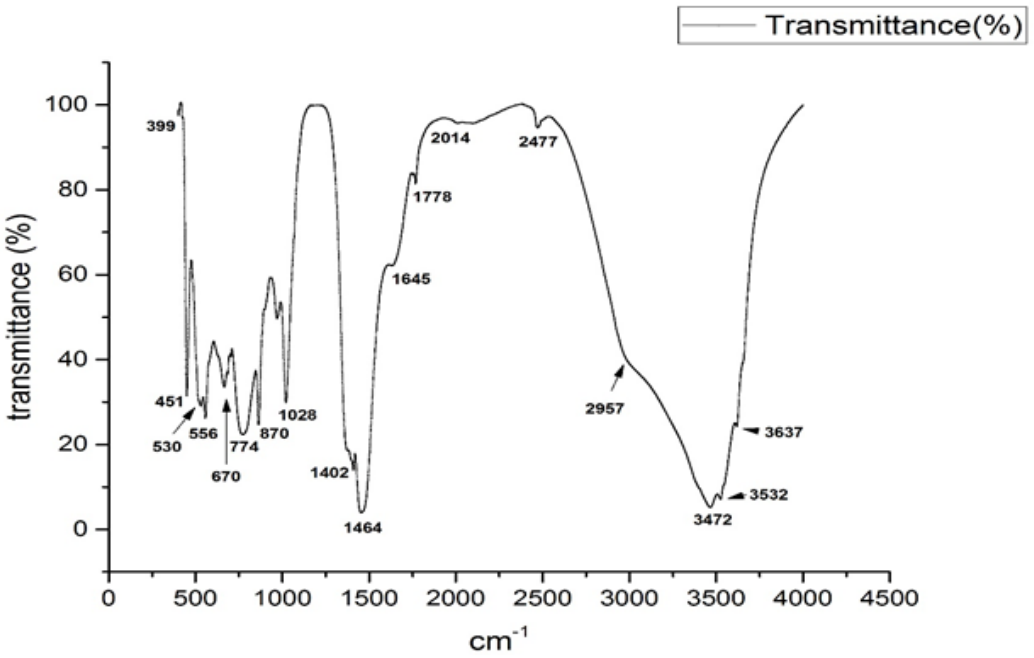

Figure 4.18: FTIR Spectra of $0.6MgO.0.4SrO.Al_2O_3$ fired at 900^OC for 3h

UV-visible Spectra

$(1-x)MgO.xSrO.Al_2O_3$ (x = 0.3, 0.4, 0.5) calcined at 900^oC and 1200^oC for 3h

The figure 4.19 shows the absorbance spectra of $(1-x)MgO.xSrO.Al_2O_3$ calcined powder in the UV-Vis region measured at room temperature. The spectrum display two wide-ranging peak at 200 nm and 250-400 nm wavelength range for $(1-x)MgO.xSrO.Al_2O_3$ (x = 0.3, 0.4, 0.5), $MgAl_2O_4$ and $SrAl_2O_4$ which was calcined at 900^oC for 3h. For $0.6MgO.0.4SrO.Al_2O_3$ which was calcined at 1200^oC for 3h, the spectrum display two wide-ranging peak and one smaller one at 300-400 nm, 250-300 nm and 200-250 nm wavelength range correspondingly. The spectrum display two wide-ranging peak which were ascend from the spin-allowed d-d conversions of Sr^{2+} ions, perceived intense peak around 250 nm could be allocated toSr^{2+} -O^{2-} charge transfer of a chromate species.

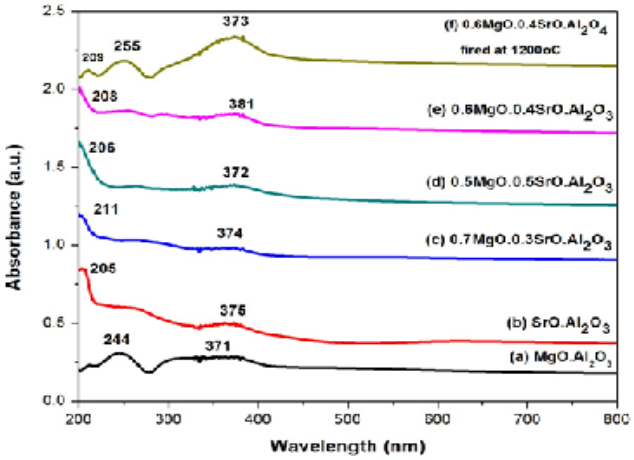

Figure 4.19: $(1-x)MgO.xSrO.Al_2O_3$ (x = 0.3, 0.4, 0.5) calcined at 900^oC and 1200^oC for 3h

Chapter 5

Conclusion

Stoichiometric composition of (1-x)$MgO.xSrO.Al_2O_3$ (x = 0.3, 0.4, 0.5)was successfully co - precipitated using metal nitrate salts and 1 molar sodium hydroxide solution at 60^oC.

XRD of the calcined powders show the formation of $MgSrAl_{10}O_{17}$ as major phase along with MgO, Al_2O_3, and $SrAl_2O_4$ as minor phase(s).

Calculated lattice parameter of $MgSrAl_{10}O_{17}$ showed good match with the standard lattice parameter(s). However, with increasing x in (1-x)$MgO.xSrO.Al_2O_3$ (x = 0.3, 0.4, 0.5), unit cell parameter a' increases and 'c' decreases suggest that c/a ratio decreases of $MgSrAl_{10}O_{17}$ in the calcined samples may end up imparting lattice strain with the neighboring minor phase(s).

SEM shows the formation nanometer sized (20-100 nm) nearly spherical crystalline agglomerate with the samples heat treated at 900°C compared to micron size particles when the temperature raised to 1200°C. Crystallite was calculated from line profile analysis from the XRD patterns using Scherrer formula showed good agreement with the particle size measured with SEM images.

References

[1] M. S. Abdi, T. Ebadzadeh, A. Ghaffari, and M. Feli, "Synthesis of nano-sized spinel (mgal 2 o 4) from short mechanochemically activated chloride precursors and its sintering behavior," *Advanced Powder Technology*, vol. 26, no. 1, pp. 175–179, 2015.

[2] L. Meng, L. Liang, and Y. Wen, "Deep red phosphors srmgal10o17: Mn4+, m (m= li+, na+, k+, cl-) for warm white light emitting diodes," *Journal of Materials Science: Materials in Electronics*, vol. 25, no. 6, pp. 2676–2681, 2014.

[3] E. N. Alvar, M. Rezaei, and H. N. Alvar, "Synthesis of mesoporous nanocrystalline mgal 2 o 4 spinel via surfactant assisted precipitation route," *Powder Technology*, vol. 198, no. 2, pp. 275–278, 2010.

[4] G.-j. Li, Z.-r. Sun, C.-h. Chen, X.-j. Cui, and R.-m. Ren, "Synthesis of nanocrystalline mgal 2 o 4 spinel powders by a novel chemical method," *Materials Letters*, vol. 61, no. 17, pp. 3585–3588, 2007.

[5] K. Y. Jung, H. W. Lee, Y. C. Kang, S. B. Park, and Y. S. Yang, "Luminescent properties of (ba, sr) mgal10o17: Mn, eu green phosphor prepared by spray pyrolysis under vuv excitation," *Chemistry of materials*, vol. 17, no. 10, pp. 2729–2734, 2005.

[6] Q.-l. Ma, B.-g. Zhai, and Y. M. Huang, "Effect of sol–gel combustion temperature on the luminescent properties of trivalent dy doped sral 2 o 4," *Ceramics International*, vol. 41, no. 4, pp. 5830–5835, 2015.

[7] P. Yang, M. K. Lü, C. F. Song, D. Xu, D. R. Yuan, G. M. Xia, and S. W. Liu, "Photoluminescence characteristics and mechanism of sral 2 o 4 co-doped with eu 3+ and cu 2+," *Inorganic Chemistry Communications*, vol. 5, no. 11, pp. 919–923, 2002.

[8] M. Ayvacıkli, Z. Kotan, E. Ekdal, Y. Karabulut, A. Canimoglu, J. G. Guinea, A. Khatab, M. Henini, and N. Can, "Solid state synthesis of sral 2 o 4: Mn 2+ co-doped with nd 3+ phosphor and its optical properties," *Journal of Luminescence*, vol. 144, pp. 128–132, 2013.

[9] H. Song, D. Chen, W. Tang, and Y. Peng, "Synthesis of sral 2 o 4: Eu 2+, dy 3+, gd 3+ phosphor by combustion method and its phosphorescence properties," *Displays*, vol. 29, no. 1, pp. 41–44, 2008.

[10] H. Du, W. Shan, L. Wang, D. Xu, H. Yin, Y. Chen, and D. Guo, "Optimization and complexing agent-assisted synthesis of green sral 2 o 4: Eu 2+, dy 3+ phosphors through sol–gel process," *Journal of Luminescence*, vol. 176, pp. 272–277, 2016.

[11] K. Pavani, J. S. Kumar, T. Sasikala, B. Jamalaiah, H. J. Seo, and L. R. Moorthy, "Luminescent characteristics of dy 3+ doped strontium magnesium aluminate phosphor for white leds," *Materials Chemistry and Physics*, vol. 129, no. 1, pp. 292–295, 2011.

[12] X. Zhiping, D. Suqing, L. Yingliang, L. Bingfu, X. Yong, and M. ZHENG, "Synthesis and luminescence properties of sral 2 o 4: Eu 2+, dy 3+ hollow microspheres via a solvothermal co-precipitation method," *Journal of Rare Earths*, vol. 31, no. 3, pp. 241–246, 2013.

[13] M. Zawrah, H. Hamaad, and S. Meky, "Synthesis and characterization of nano mgal 2 o 4 spinel by the co-precipitated method," *Ceramics International*, vol. 33, no. 6, pp. 969–978, 2007.

[14] Z. Xue, S. Deng, and Y. Liu, "Synthesis and luminescence properties of sral 2 o 4: Eu 2+, dy 3+ nanosheets," *Physica B: Condensed Matter*, vol. 407, no. 18, pp. 3808–3812, 2012.

[15] D.-S. Xing, K.-W. Cheah, P.-Y. Cheng, J. Xu, J.-X. Shi, H.-B. Liang, and M.-L. Gong, "A novel blue magnesium strontium aluminate-based phosphor for pdp application," *Solid state communications*, vol. 134, no. 12, pp. 809–813, 2005.

[16] V. Singh, T. G. Rao, and J.-J. Zhu, "A rapid combustion process for the preparation of mgsral 10 o 17: Eu 2+ phosphor and related luminescence and defect investigations," *Journal of Luminescence*, vol. 128, no. 4, pp. 583–588, 2008.

[17] V. Singh, R. Chakradhar, J. Rao, and D.-K. Kim, "Mn 2+ activated mgsral 10 o 17 green-emitting phosphor—a luminescence and epr study," *Journal of Luminescence*, vol. 128, no. 9, pp. 1474–1478, 2008.

[18] V. Singh, S. Watanabe, T. G. Rao, J. F. D. Chubaci, and H.-Y. Kwak, "Luminescence and defect centres in mgsral 10 o 17: Sm 3+ phosphor," *Journal of Non-Crystalline Solids*, vol. 356, no. 23, pp. 1185–1190, 2010.

[19] V. Pawade and S. Dhoble, "Blue emission in eu 2+ activated mgxal 10 o 17 (x= sr, ca) phosphors," *Optik-International Journal for Light and Electron Optics*, vol. 123, no. 20, pp. 1879–1883, 2012.

[20] V. Singh, V. K. Rai, V. Venkatramu, R. Chakradhar, and S. H. Kim, "Infrared emissions in mgsral 10 o 17: Er 3+ phosphor co-doped with yb 3+/ba 2+/ca 2+ obtained by solution combustion route," *Journal of Luminescence*, vol. 134, pp. 396–400, 2013.

[21] G. Ju, Y. Hu, L. Chen, and X. Wang, "Photoluminescence properties of color-tunable srmgal 10 o 17: Eu 2+, mn 2+ phosphors for uv leds," *Journal of Luminescence*, vol. 132, no. 7, pp. 1792–1797, 2012.

[22] V. Singh, R. Chakradhar, J. Rao, and S. Kim, "Epr and luminescence studies of cr 3+ doped mgsral 10 o 17 phosphor synthesized by a low-temperature solution combustion route," *Journal of Luminescence*, vol. 154, pp. 328–333, 2014.

[23] L. Wang, H. Zhang, Y. Li, P. Liang, Y. Shen, and F. Jiao, "Enhanced luminescence in the srmgal10o17: Eu2+ blue phosphor prepared by a hybrid urea-sol combustion route," *International Journal of Applied Ceramic Technology*, vol. 13, no. 1, pp. 185–190, 2016.

[24] S. Tigga, N. Brahme, and D. Bisen, "Effect of gamma irradiation on thermoluminescence and fracto-mechanoluminescence properties of srmgal 10 o 17: Eu 2+ phosphor," *Optical Materials*, vol. 53, pp. 109–115, 2016.